https://doi.org/10.5194/essd-2025-277
Preprint. Discussion started: 10 June 2025

A Bioavailable Strontium Isoscape of Australia

Anthony Dosseto[1], Florian Dux[1], Clément Bataille[2,3,] Patrice de Caritat[4,5]

[1]Wollongong Isotope Geochronology Laboratory, Environmental Futures, School of Science, University of Wollongong, Wollongong NSW 2522, Australia
[2]University of Ottawa, Earth and Environmental Sciences, Ottawa, Canada
3 Purdue University, Forestry and Natural Resources, West Lafayette, Indiana, USA
[4]Geoscience Australia, GPO Box 378, Canberra ACT 2601, Australia
[5]John de Laeter Centre, Curtin University, Bentley WA 6102, Australia

Correspondence to: Anthony Dosseto (tonyd@uow.edu.au)

Abstract

Strontium isotope ratios ($^{87}Sr/^{86}Sr$) at the Earth's surface offer powerful tools for geological, environmental, and archaeological applications. In minerals and biological materials, $^{87}Sr/^{86}Sr$ reflects the isotopic composition of the local bedrock and derived soils. In Australia, however, large regional-scale surveys of bioavailable $^{87}Sr/^{86}Sr$ remain scarce. Here, we present a new dataset of bioavailable $^{87}Sr/^{86}Sr$ ratios from 278 catchment outlet (floodplain) sediment samples, spanning inland southeastern Australia (South Australia, New South Wales, Victoria), northern Western Australia, the Northern Territory, Queensland (north of 21.5°S), and the Yilgarn Craton in southern Western Australia. Combined with more than 20,000 global Sr isotope measurements, this dataset was used to generate a high-resolution isoscape of Australia using random forest regression (Bataille et al., 2020).

Australian bioavailable $^{87}Sr/^{86}Sr$ values span a narrower range (0.70501–0.78121) compared to co-located bulk sediment values (0.70480–1.09089) (Caritat et al., 2022, 2023, 2025b), reflecting the influence of soluble and exchangeable mineral phases and atmospheric inputs such as rain and dust. The predicted isoscape reproduces major geological patterns, with higher values over ancient crustal provinces like the Yilgarn Craton and eastern Palaeozoic orogens, and lower values across younger sedimentary basins and coastal margins. Model uncertainty, assessed via prediction standard deviations, is lowest across well-sampled, geologically stable regions and highest in coastal and lithologically complex zones. Compared to existing global and regional isoscapes, our model offers significantly improved coverage and resolution for Australia. This isoscape provides a robust baseline for applications in provenance research, palaeoecology, and environmental geochemistry.

1 Introduction

Provenancing—the ability to trace the geographic origin of materials—is a vital tool across disciplines such as ecology, archaeology, food authentication, and forensic science. In Australia, this capability is particularly valuable due to the

https://doi.org/10.5194/essd-2025-277
Preprint. Discussion started: 10 June 2025

continent's unique biogeography, ancient human history, and significant food production systems. Australia's ecosystems have evolved in isolation, resulting in many endemic species with region-specific foraging or migration behaviours. Understanding the ecological histories of both extant and extinct fauna necessitates geochemical tools capable of linking individuals to specific landscapes. Similarly, tracing the origin and movement of archaeological materials and human remains is fundamental to understanding the peopling of Australia, the development of long-distance trade routes, and the complex land-use practices of Aboriginal peoples. In contemporary applications, provenance tools are increasingly used to verify the geographic origin of agricultural commodities—such as wine, seafood, and grain—important both for biosecurity and for protecting the reputation of high-value Australian exports. Despite these diverse applications, there remains a critical limitation: Australia lacks a continent-scale framework for biologically relevant isotopic provenancing.

The strontium (Sr) isotope ratio ($^{87}Sr/^{86}Sr$) is a powerful tool used across a wide range of disciplines, including geoscience, palaeoecology, archaeology, and forensic science. In geoscience, $^{87}Sr/^{86}Sr$ ratios are applied to investigate processes such as continental weathering, sediment provenance, and the evolution of crustal materials over geological time (e.g. Bataille et al., 2020; Mcnutt, 2000). In archaeology and forensic science, variations in $^{87}Sr/^{86}Sr$ have been used to trace the origin of artefacts, human remains, and food products by linking them to specific geological regions (e.g. Frei and Frei, 2013; Willmes et al., 2014; Voerkelius et al., 2010). This broad applicability stems from the fact that $^{87}Sr/^{86}Sr$ ratios remain stable during biological and chemical processes, preserving the isotopic signature of the original environment (Gosz et al., 1983; Nebel and Stammeier, 2018).

The $^{87}Sr/^{86}Sr$ ratio of a material varies across the landscape due to differences in the age and rubidium (Rb) content of underlying rocks. Older rocks, particularly those rich in Rb, such as granites and metamorphic rocks, tend to have higher $^{87}Sr/^{86}Sr$ ratios, whereas younger volcanic rocks and carbonates typically display lower values (e.g. Bataille et al., 2020; Mcnutt, 2000). Weathering of these rocks releases Sr into soils, waters, and vegetation, transferring the distinct isotopic signatures to the biosphere. This natural variation enables researchers to map $^{87}Sr/^{86}Sr$ distributions across regions ("isoscapes") and use these maps to infer the provenance of materials, reconstruct past human and animal movements, and investigate environmental and geological processes (e.g. Bataille et al., 2018; Caritat et al., 2023).

When using Sr isotopes as a provenance tool, a well-constrained Sr isoscape is essential (Hobson et al., 2010). Although a few efforts have been made to develop Sr isoscapes in Australia, existing datasets remain limited in spatial coverage or relevance for biological provenancing. The study by Adams et al. (2019) covers only a small portion of the continent across the Cape York Peninsula, while Caritat et al. (2022, 2023, 2025b) provide $^{87}Sr/^{86}Sr$ data for bulk sediment across inland southeastern, northern Australia, and the Yilgarn Craton, respectively. However, provenance studies in archaeology, forensic science, and palaeoecology are based on comparing biological tissues of unknown origin with the isotopic composition of bioavailable Sr—the fraction accessible to plants and animals—rather than bulk or total sediment Sr (Bataille et al., 2020; Capo et al., 1998). Bioavailable Sr more accurately reflects the isotopic signature incorporated into biological tissues, making it critical for robust provenance interpretations in these fields.

https://doi.org/10.5194/essd-2025-277
Preprint. Discussion started: 10 June 2025

The aim of this study is to develop the first continent-scale isoscape of bioavailable $^{87}Sr/^{86}Sr$ for Australia. We generated a new dataset of bioavailable Sr isotope ratios from 278 catchment outlet sediment samples, spanning a range of climatic zones and geological provinces across the continent. These data were integrated with a global compilation of >20,000 plant, soil, and water Sr isotope ratios—including an additional 292 georeferenced samples from Australia—to train a random forest regression model, enabling spatial prediction of bioavailable $^{87}Sr/^{86}Sr$ values across unsampled regions. The resulting isoscape provides a preliminary, geochemically informed, spatially continuous framework to support provenance research in archaeological, ecological, and forensic contexts. By addressing the current lack of bioavailable Sr data for Australia, this study enhances the application of isotope-based provenancing across diverse environmental and cultural landscapes.

2 Study Area

This study focuses on terrestrial samples collected across northern, southeastern, and western Australia as part of the National Geochemical Survey of Australia (NGSA) project (Caritat and Cooper, 2011; Caritat and Cooper, 2016; Caritat et al., 2022). The NGSA aimed to provide a consistent geochemical baseline for the Australian continent by sampling fine-grained fluvial and alluvial sediments near major catchment outlets (Caritat and Cooper, 2011). The selected catchments vary widely in climate, geology, and landscape history, spanning tropical, semi-arid, and temperate zones.

In northern Australia, catchments are dominated by deeply weathered Precambrian bedrock, including granites, gneisses, and Proterozoic sedimentary rocks, overprinted by extensive regolith development (Caritat et al., 2023). Southeastern Australia features a mix of Palaeozoic granites, volcanic provinces, and younger sedimentary basins (Caritat et al., 2022). Western Australia, particularly the Yilgarn Craton, represents some of the oldest continental crust on Earth, consisting mainly of Archean granite-greenstone terranes and Proterozoic basins (Caritat et al., 2025b).

The sampled areas are generally characterised by minimal recent glaciation or rejuvenation, resulting in thick, stable weathering profiles (Wilford, 2012). In many locations, aeolian processes contribute to sediment mixing, particularly in arid and semi-arid regions (Caritat and Cooper, 2011). Catchment outlet sediments therefore integrate signals from diverse lithological sources, modified by long-term weathering and surface processes.

Bioavailable Sr isotope ratios ($^{87}Sr/^{86}Sr$) were measured on the <2 mm fraction of these sediments to characterise the isotopic landscape ("isoscape") at a continental scale. While sampling density (~1 site per 5,200 km²) limits fine-scale spatial resolution, the large coverage provides a robust first-order framework for provenance and environmental studies across much of Australia.

3 Material and methods

3.1 Material

This study makes use of archived sediment samples collected by the National Geochemical Survey of Australia (NGSA), a continental-scale geochemical mapping program that systematically sampled catchment outlet sediments across approximately 80% of the Australian landmass (Caritat and Cooper, 2011). A summary of the NGSA results and impact has been presented by De Caritat (2022). The NGSA targeted fine-grained fluvial and alluvial sediments at major catchment outlets, which serve as effective integrators of upstream geological inputs through natural weathering and sediment transport. Sampling was conducted at an ultralow density of approximately one site per 5,200 km^2, designed to capture large-scale geochemical variation across diverse climatic and geological regions. This approach follows protocols adopted in other national-scale surveys (e.g. Ottesen et al., 1989; Bølviken et al., 2004).

For the present study, we selected 278 NGSA samples from across northern, southeastern, and western Australia (Figure 1), prioritising areas not previously covered by bioavailable Sr isotope analysis, but previously studied for bulk Sr isotopes. These samples underpin the development of the first continental-scale isoscape of bioavailable $^{87}Sr/^{86}Sr$ in Australia. The catchment outlet sediments share characteristics with floodplain deposits, being deposited during receding floodwaters, but also reflect aeolian influences in some regions. The sampled settings were typically vegetated and biologically active, with soils forming on transported alluvial parent material.

In contrast to the bulk Sr isotope ratios reported in Caritat et al. (2022, 2023, 2025b), the bioavailable Sr was extracted from the <2 mm fraction of 'top outlet sediment' (TOS) samples (Caritat et al., 2025a). The TOS samples were taken from shallow pits at ~0.1 m depth (Lech et al., 2007). In the laboratory, samples were air-dried, milled, and processed following documented NGSA protocols (Caritat et al., 2010). While the low sampling density constrains fine-scale resolution, the broad spatial coverage provides a valuable baseline for Sr isotopic variation and supports future provenance, palaeoenvironmental, and landscape evolution studies.

3.2 Methods

Samples were prepared and analysed for $^{87}Sr/^{86}Sr$ ratios at the Wollongong Isotope Geochronology Laboratory (WIGL). Bioavailable Sr was extracted from the <2 mm fraction of sediment samples using a 1 M ammonium acetate (NH_4OAc) leach at pH 7, targeting the exchangeable and readily soluble Sr fraction (Moffat et al., 2020). Approximately 1 g of dried, milled sample was weighed into a 15 mL polypropylene tube and leached with 2.5 mL of the NH_4OAc solution for 24 hours on a table shaker at 3000 rpm. Following leaching, the supernatant was filtered through a 0.45 µm PTFE syringe filter to remove particulates and organic material.

The filtered leachate was evaporated to incipient dryness on a hotplate at 100 °C, then re-dissolved in 2 mL of 2 M HNO_3. A 1:100 dilution in 0.3 M HNO_3 was prepared from each sample to screen for Sr concentration prior to chromatographic

https://doi.org/10.5194/essd-2025-277
Preprint. Discussion started: 10 June 2025

separation. Strontium was separated from the sample matrix using an automated low-pressure chromatographic system (Elemental Scientific prepFAST-MC™) equipped with 1 mL Sr–Ca resin columns (Eichrom™), following the procedure of Romaniello et al. (2015). Purified Sr fractions were collected and re-dissolved in 0.3 M HNO_3 prior to isotope ratio analysis. Strontium isotope ratios were measured using a Thermo Scientific Neptune Plus multi-collector inductively coupled plasma mass spectrometer (MC-ICP-MS) at WIGL. Samples were introduced via an ESI Apex-ST PFA MicroFlow nebuliser (~0.1 mL min^{-1} uptake rate) coupled to an SSI quartz dual cyclonic spray chamber, with a jet sample cone and X-skimmer cone configuration. Analyses were performed in low-resolution mode. Instrument tuning was conducted at the start of each analytical session using a 20 ppb Sr solution, with typical ^{88}Sr signal intensities of ~4 V. Isotopes ^{88}Sr, ^{87}Sr, ^{86}Sr, ^{85}Rb, ^{84}Sr, and ^{83}Kr were collected simultaneously on Faraday detectors. Instrumental mass bias was corrected using internal normalisation of ^{87}Sr/^{86}Sr to the known ^{88}Sr/^{86}Sr ratio via the exponential law. Isobaric interferences from ^{87}Rb and ^{86}Kr were corrected using intensities measured at masses 85 and 83, respectively.

The National Institute of Standards and Technology (NIST) strontium carbonate isotope Standard Reference Material SRM987 was used as a secondary standard and analysed after every five samples to monitor instrument stability and analytical accuracy. However, full procedural accuracy—encompassing leaching, filtration, and chromatographic separation—could not be assessed due to the lack of an appropriate certified reference material that undergoes the same sample preparation steps as the sediment leachates. No standard reference material currently exists that replicates the matrix and leaching behaviour of ammonium acetate-extractable bioavailable Sr. As such, while instrumental accuracy is constrained by SRM987, the potential for matrix-specific biases or fractionation during leaching could not be independently verified.

To assess analytical reproducibility, a total of ten field duplicates were independently leached, processed, and analysed for ^{87}Sr/^{86}Sr. These replicate pairs span the full range of observed values in the dataset. Paired results show excellent reproducibility, with differences between replicates ranging from ±0.00003 to ±0.00015, and an average absolute difference of 0.000043 (median = 0.000030). These results are consistent with those reported in similar studies using NH_4OAc extraction and MC-ICP-MS analysis (e.g. Moffat et al., 2020). Precision based on 2 standard errors ranged from ±0.000007 to ±0.000036 across replicates, reflecting both analytical performance and micro-scale sediment heterogeneity. Total procedural blanks were low, ranging from 0.07 to 0.26 ng Sr (n = 8), and are negligible relative to sample Sr concentrations. Overall, the quality of the ^{87}Sr/^{86}Sr dataset is considered appropriate for regional-scale isoscape modelling. Given the level of analytical precision observed, we report ^{87}Sr/^{86}Sr values to the fifth decimal place. Replicate measurements show differences within acceptable limits, and no significant additional variation is observed among field duplicates beyond that attributable to sample heterogeneity and standard analytical uncertainty.

https://doi.org/10.5194/essd-2025-277
Preprint. Discussion started: 10 June 2025

3.3 Strontium Isoscape Calculation

The Sr isoscape was generated using the random forest regression model approach described by Bataille et al. (2020). In addition to the 278 bioavailable $^{87}Sr/^{86}Sr$ measurements from Australian sediment leachates reported in this study, the model was trained on a global dataset of >20,000 Sr isotope measurements derived from plant tissues, soil exchangeable fractions, and water samples—including 292 additional samples from Australia. This combined dataset captures a wide range of geological and environmental settings, improving the generalisability of the model.

The model incorporates 26 geospatial predictor variables representing geological, climatic, soil, hydrological, and vegetation attributes (see Table 1). This integration of Sr isotope observations with environmental covariates enables the prediction of bioavailable $^{87}Sr/^{86}Sr$ values across unsampled regions, producing a continuous spatial model of Sr isotopic variation at a resolution of approximately 0.03° × 0.025° (~3 km × 2.5 km).

In addition to predicted values, the model outputs a spatial layer of standard deviations (SD), which quantifies the uncertainty of $^{87}Sr/^{86}Sr$ predictions across the landscape. Areas with low SD values indicate high model confidence—often reflecting well-characterised environmental conditions or strong covariate signal—while higher SD values highlight regions where predictions are more uncertain due to environmental complexity or sparse training data.

4 Results

4.1 Bioavailable and Bulk $^{87}Sr/^{86}Sr$ Distributions

Bioavailable $^{87}Sr/^{86}Sr$ ratios in the Australian sediment samples range from 0.70501 to 0.78121, with a mean of 0.72131 (Caritat et al., 2025a). Distinct regional patterns are evident (Figure 2; Table 1). Samples from southeastern Australia (South Australia, New South Wales, Victoria) display the lowest mean $^{87}Sr/^{86}Sr$ (0.71277), with values ranging from 0.70739 to 0.71908. In contrast, samples from northern Australia (Northern Territory, northern Western Australia, and Queensland north of 21.5°S) exhibit a higher mean of 0.72150 and a broader isotopic range (0.70501–0.78121), reflecting more heterogeneous and complex geology. Sediments from southwestern Australia (Yilgarn Craton) are more radiogenic overall, with a mean $^{87}Sr/^{86}Sr$ of 0.72468 and values ranging from 0.71153 to 0.75274.

In comparison, bulk sediment $^{87}Sr/^{86}Sr$ values, taken on milled and co-located sediment samples, are systematically higher and more variable, spanning from 0.7048 to 1.0909 (mean = 0.7501; Table 1) (Caritat et al., 2025b). Across all regions, bioavailable Sr is consistently less radiogenic than bulk Sr (Figure 3; Figure 4). The average offset between bioavailable and co-located bulk $^{87}Sr/^{86}Sr$ values is approximately:

- 0.010 in southeastern Australia,
- 0.028 in northern Australia,
- 0.040 in southwestern Australia.

https://doi.org/10.5194/essd-2025-277
Preprint. Discussion started: 10 June 2025

This systematic difference reflects the distinct geochemical behaviour of Sr in different sediment fractions. The broader range in bulk sediments results from the inclusion of radiogenic minerals such as feldspars and micas, while the bioavailable fraction—primarily derived from weathered, exchangeable, or soluble phases and atmospheric inputs such as rainwater and dust—exhibits a narrower range. These differences are driven by the nature of the source material and are not attributable to differences in sample count (n = 576 for bulk, n = 278 for bioavailable). The distributions are summarised in Figure 3, and individual paired comparisons are shown in Figure 4.

4.2 Predicted Isoscape and Regional Patterns

The bioavailable $^{87}Sr/^{86}Sr$ isoscape of Australia was generated using a random forest regression model trained on the 278 sediment samples from this study and supplemented by over 20,000 global Sr isotope values (see Section 3.3). The resulting model predicts broad-scale isotopic variation that aligns with major geological provinces (Figure 5; Supplementary Material). Elevated $^{87}Sr/^{86}Sr$ values are predicted over the Yilgarn Craton and parts of eastern Australia, consistent with ancient Archean and Palaeozoic bedrock. In contrast, younger sedimentary basins of central and northern Australia show lower predicted values. Coastal areas, particularly in northern and northwestern Australia, also exhibit low $^{87}Sr/^{86}Sr$ values, possibly influenced by sea salt aerosols and recent sediments. These regional patterns mirror Australia's lithological and climatic gradients and confirm the strong geological control on the bioavailable Sr pool.

4.3 Prediction Uncertainty

A map of standard deviation (SD) values was generated to assess model uncertainty (Figure 6; Supplementary Material). Prediction uncertainty is lowest (SD < 0.003) across geologically stable and environmentally homogeneous regions, particularly in central and western Australia. In some of these areas, especially central Australia, low uncertainty reflects consistent and well-constrained covariate values in the model (e.g. bedrock Sr isotope composition, dust inputs), even where empirical bioavailable $^{87}Sr/^{86}Sr$ measurements are sparse or absent. In contrast, higher uncertainty (SD > 0.005) occurs in geologically complex or environmentally variable regions such as coastal northern Australia, eastern Australia, and Tasmania, where model extrapolations are less constrained by training data. This SD map should serve as an important tool for interpreting prediction reliability and for guiding future sampling efforts.

4.4 Model Performance and Variable Importance

Cross-validation of the global random forest model yielded an R^2 of 0.473, RMSE of 0.0100, and MAE of 0.00310, reflecting moderate predictive performance across diverse global environments. While these values reflect model fit at the global scale, regional performance within Australia may differ depending on sampling density and local geological complexity. Variable importance analysis using the VSURF (Variable Selection Using Random Forests) algorithm (Genuer et al., 2010) identified five key predictors influencing the global model of bioavailable $^{87}Sr/^{86}Sr$: median bedrock $^{87}Sr/^{86}Sr$

https://doi.org/10.5194/essd-2025-277
Preprint. Discussion started: 10 June 2025

values, maximum geological age, simulated dust source distance, mean terrane age, and mean annual precipitation. These variables were selected based on their contribution to reducing model prediction error across the global training dataset. The results highlight the dominant role of geological composition and crustal evolution in shaping bioavailable Sr isotope variation, with additional influence from atmospheric and climatic processes. While the model was globally trained, the inclusion of variables such as dust transport and precipitation is consistent with known Sr cycling mechanisms in Australia, where aeolian deposition and climate gradients significantly affect the mobile Sr pool.

5 Discussion

This study presents a new machine learning-based isoscape of bioavailable $^{87}Sr/^{86}Sr$ for Australia, generated using a random forest model trained on 278 sediment samples and supplemented with over 20,000 global Sr isotope data points, including Australian bioavailable Sr isotope data from Adams et al. (2019). The resulting isoscape represents the most comprehensive spatial prediction of bioavailable Sr isotopic variation to date for the continent, with broad implications for geochemical, archaeological, ecological, and forensic applications. The spatial distribution of predicted $^{87}Sr/^{86}Sr$ values closely reflects the geological architecture of the Australian continent. Higher ratios correspond with older crustal provinces, notably the Archean Yilgarn Craton and Palaeozoic orogens in eastern Australia, while lower ratios are associated with younger sedimentary basins, coastal plains, and regions influenced by marine or aeolian inputs. These patterns are consistent with established geochemical principles whereby radiogenic ^{87}Sr accumulates over time in Rb-rich lithologies such as granites and gneisses (Faure and Powell, 2012), and less radiogenic values are found in mafic, carbonate, or younger siliciclastic environments (Bataille et al., 2020; Willmes et al., 2018).

The key predictors identified by the VSURF analysis—median bedrock $^{87}Sr/^{86}Sr$, geological age, simulated dust source distance, mean terrane age, and mean annual precipitation—reflect globally important controls on bioavailable Sr isotope variation. The prominence of geological variables is consistent with well-established geochemical principles: older, Rb-rich lithologies typically contribute more radiogenic $^{87}Sr/^{86}Sr$ signatures to soils and sediments. The inclusion of atmospheric and climatic variables such as dust transport distance and precipitation highlights the broader environmental processes that can influence the mobile Sr pool, particularly through aeolian and hydrological redistribution. While the model was trained on a global dataset, these results are geochemically plausible in the Australian context, where low-relief, deeply weathered landscapes and dust transport are key features (Wilford, 2012; Caritat et al., 2022). The findings underscore the importance of incorporating both geological and surface process variables when predicting bioavailable Sr, especially in regions with extensive regolith cover or where external inputs may obscure local bedrock signals (Bataille & Bowen, 2012).

Prediction uncertainty, visualised through the SD map, shows lowest uncertainty across geologically simple and well-sampled regions of western Australia. In contrast, higher uncertainties (>0.005) occur in coastal northern Australia, eastern highlands, and Tasmania—areas with more variable lithologies, sparse sampling, or environmental heterogeneity. Following recommendations from Willmes et al. (2018) and Scaffidi and Knudson (2020), we emphasise that users of the isoscape

https://doi.org/10.5194/essd-2025-277
Preprint. Discussion started: 10 June 2025

Open Access Earth System Science Data Discussions

should carefully consider local uncertainty when applying it to provenance assignments or ecological interpretations. Spatially variable prediction confidence is particularly important in forensic and archaeological contexts, where assignment errors can lead to misinterpretation of individual mobility or material origin.

Compared to existing Sr isoscapes, this study substantially improves both the spatial coverage and resolution of bioavailable $^{87}Sr/^{86}Sr$ predictions for Australia. The regional isoscape developed by Adams et al. (2019) for the Cape York Peninsula represented a foundational effort in biologically relevant Sr modelling in Australia, based on direct measurements from plant, water, and soil leachates. However, its geographic scope was limited to ~300,000 km² in northeastern Australia, constraining its broader applicability. The high-resolution isoscape for France by Willmes et al. (2018) demonstrated the value of integrating geological and environmental covariates in a spatial modelling framework, but was developed and calibrated for a European context. The global isoscape by Bataille et al. (2020) provided valuable continental-scale predictions, yet relied on sparse empirical data from Australia and extensive extrapolation over unsampled areas.

The present study addresses this gap by generating the first continent-wide bioavailable $^{87}Sr/^{86}Sr$ isoscape for Australia, based on 278 new sediment leachate measurements integrated into a globally trained machine learning model. This approach increases the empirical representation of Australian geochemical landscapes and provides a robust spatial baseline for provenance, ecological, and archaeological applications. At a regional level, our predicted values for Cape York are consistent with spatial trends reported by Adams et al. (2019), including lower values over western sediments and higher values associated with older basement lithologies in the east. However, our predicted values are systematically ~0.003–0.005 lower, likely due to differences in sampling media (sediment leachates versus in situ biological samples) and the spatial smoothing inherent to machine learning predictions.

Despite its advances, the model has limitations. The input data are derived from sediment <2 mm fractions, which, while practical and regionally representative, may not fully capture the Sr accessible to plants, animals, or humans (Copeland et al., 2016; Bataille et al., 2020). The model performance, assessed globally (R^2 = 0.473, RMSE = 0.0100), reflects moderate accuracy but could vary regionally. The spatial resolution is limited by the original NGSA sampling density (~1 site per 5,200 km²), and some areas—particularly the interior of northern Australia and Tasmania—remain undersampled or uncertain. Additionally, local processes such as fertiliser use, hydrological inputs, or vegetation type can alter the bioavailable Sr signature but are not explicitly included in the model. Nonetheless, the isoscape provides a valuable foundation for a wide range of provenance and landscape-scale applications. Its integration of global training data and robust environmental covariates allows for flexible application in regions where local Sr datasets are scarce. Future improvements could involve the integration of additional isotope systems (e.g., O, Pb, C) as demonstrated in other provenancing studies (e.g. Evans et al., 2006; Bataille et al., 2021), allowing for more refined geographic assignments and greater resolution in complex settings. Expanding plant- and water-based bioavailable Sr datasets across underrepresented regions of Australia, including use the rest of the NGSA sample set, would further enhance the spatial accuracy and interpretive value of this model.

https://doi.org/10.5194/essd-2025-277
Preprint. Discussion started: 10 June 2025

Open Access Earth System Science Data Discussions

6 Conclusions

This study presents the first machine learning-based isoscape of bioavailable strontium isotope ($^{87}Sr/^{86}Sr$) ratios across large parts of Australia. By integrating 278 sediment-derived Sr isotope measurements with global datasets of plants, soils, and waters, and using a random forest regression model, we produced a continuous spatial prediction of Sr isotope variation at the continental scale.

The isoscape captures major geological controls, with higher $^{87}Sr/^{86}Sr$ values associated with ancient terrains such as the Yilgarn Craton and Palaeozoic provinces of eastern Australia, and lower values over younger sedimentary basins and coastal regions. Variable selection analysis identified bedrock $^{87}Sr/^{86}Sr$ values, geological age, dust source distance, terrane age, and precipitation as key predictors. An associated SD map highlights areas of higher uncertainty, particularly along coastal margins and in regions with complex geology.

Comparison with previous regional and global Sr isoscapes confirms that our model reliably reproduces broad isotopic patterns while providing significantly improved coverage for Australia. Although limitations remain due to sampling density and the use of sedimentary proxies, the resulting isoscape offers an important new baseline for provenance research, palaeoecological reconstructions, and environmental applications. Future work should focus on expanding bioavailable sampling coverage and refining models at finer spatial scales.

Author contributions. AD provided technical guidance, resources, supervision, data curation, and led the analysis, visualisation, and manuscript writing. FD produced the Sr isotope data and assisted with data curation. CB contributed to the isoscape calculation and assisted with manuscript editing. PdC conceived the study, provided samples and funding, contributed to data curation, and assisted with manuscript editing.

Competing interests. The contact author has declared that none of the authors has any competing interests.

Disclaimer. PdC publishes with the permission from the Chief Executive Officer, Geoscience Australia.

Data availability. The bioavailable Sr isotope dataset is available from the Geoscience Australia e-Catalogue entry by Caritat et al. (2025a) on https://dx.doi.org/10.26186/150024 and can be visualised on the Geoscience Australia Data Portal on https;//TBA.

Acknowledgments The National Geochemical Survey of Australia (NGSA) was made possible through Commonwealth funding provided by the Onshore Energy Security Program and Geoscience Australia appropriation funding (http://www.ga.gov.au/ngsa). We gratefully acknowledge the collaboration of geoscience agencies from all Australian states and the Northern Territory. We thank all landowners and custodians—private, corporate, and traditional—for granting

https://doi.org/10.5194/essd-2025-277
Preprint. Discussion started: 10 June 2025

access to sampling sites. We also acknowledge the support of Geoscience Australia laboratory staff for their assistance with sample preparation.

References

Adams, S., Grün, R., McGahan, D., Zhao, J.-X., Feng, Y., Nguyen, A., Willmes, M., Quaresimin, M., Lobsey, B., Collard, M., and Westaway, M. C.: A strontium isoscape of north-east Australia for human provenance and repatriation, Geoarchaeology, https://doi.org/10.1002/gea.21728, 2019.

Bataille, C. P., Crowley, B. E., Wooller, M. J., and Bowen, G. J.: Advances in global bioavailable strontium isoscapes, Palaeogeography, Palaeoclimatology, Palaeoecology, 555, 109849, https://doi.org/10.1016/j.palaeo.2020.109849, 2020.

Bataille, C. P., von Holstein, I. C., Laffoon, J. E., Willmes, M., Liu, X.-M., and Davies, G. R.: A bioavailable strontium isoscape for Western Europe: A machine learning approach, PloS one, 13, e0197386, https://doi.org/10.1371/journal.pone.0197386, 2018.

Bataille, C. P., Jaouen, K., Milano, S., Trost, M., Steinbrenner, S., Crubezy, E., and Colleter, R.: Triple sulfur-oxygen-strontium isotopes probabilistic geographic assignment of archaeological remains using a novel sulfur isoscape of western Europe, PLoS One, 16, e0250383, https://doi.org/10.1371/journal.pone.0250383, 2021.

Bølviken, B., Bogen, J., Jartun, M., Langedal, M., Ottesen, R., and Volden, T.: Overbank sediments: a natural bed blending sampling medium for large—scale geochemical mapping, Chemometrics and Intelligent Laboratory Systems, 74, 183-199, https://doi.org/10.1016/j.chemolab.2004.06.006, 2004.

Capo, R. C., Stewart, B. W., and Chadwick, O. A.: Strontium isotopes as tracers of ecosystem processes: theory and methods, Geoderma, 82, 197-225, https://doi.org/10.1016/S0016-7061(97)00102-X, 1998.

Caritat, P. d. and Cooper, M.: National geochemical survey of Australia: the geochemical atlas of Australia, Geoscience Australia Canberra, https://doi.org/10.11636/Record.2011.020, 2011.

Caritat, P. d. and Cooper, M. L.: A continental-scale geochemical atlas for resource exploration and environmental management: the National Geochemical Survey of Australia, https://doi.org/10.1144/geochem2014-322,

Caritat, P. d., Dosseto, A., and Dux, F.: A bioavailable strontium isoscape of Australia: initial contribution, https://doi.org/10.26186/150024, 2025a.

Caritat, P. d., Dosseto, A., and Dux, F. W.: A strontium isoscape of inland southeastern Australia, Earth System Science Data, https://doi.org/10.5194/essd-14-4271-2022, 2022.

Caritat, P. d., Dosseto, A., and Dux, F. W.: A strontium isoscape of northern Australia, Earth Syst. Sci. Data Discuss., 2023, 1-32, https://doi.org/10.5194/essd-15-1655-2023, 2023.

Caritat, P. d., Dosseto, A., and Dux, F. W.: A strontium isoscape of southwestern Australia and progress toward a national strontium isoscape, Earth Syst. Sci. Data, 17, 79-93, https://doi.org/10.5194/essd-17-79-2025, 2025b.

Caritat, P. d., Cooper, M., Pappas, W., Thun, C., and Webber, E.: National Geochemical Survey of Australia: Analytical Methods Manual, 2010.

Copeland, S. R., Cawthra, H. C., Fisher, E. C., Lee-Thorp, J. A., Cowling, R. M., le Roux, P. J., Hodgkins, J., and Marean, C. W.: Strontium isotope investigation of ungulate movement patterns on the Pleistocene Paleo-Agulhas Plain of the Greater Cape Floristic Region, South Africa, Quaternary Science Reviews, 141, 65-84, https://doi.org/10.1016/j.quascirev.2016.04.002, 2016.

de Caritat, P.: The National Geochemical Survey of Australia: review and impact, Geochemistry: Exploration, Environment, Analysis, 22, https://doi.org/10.1144/geochem2022-032, 2022.

Evans, J., Stoodley, N., and Chenery, C.: A strontium and oxygen isotope assessment of a possible fourth century immigrant population in a Hampshire cemetery, southern England, Journal of Archaeological Science, 33, 265-272, https://doi.org/10.1016/j.jas.2005.07.011, 2006.

Faure, G. and Powell, J. L.: Strontium isotope geology, Springer Science & Business Media2012.

Frei, R. and Frei, K. M.: The geographic distribution of Sr isotopes from surface waters and soil extracts over the island of Bornholm (Denmark)–A base for provenance studies in archaeology and agriculture, Applied Geochemistry, 38, 147-160, https://doi.org/10.1016/j.apgeochem.2013.09.007, 2013.

Genuer, R., Poggi, J.-M., and Tuleau-Malot, C.: Variable selection using random forests, Pattern Recognition Letters, 31, 2225-2236, https://doi.org/10.1016/j.patrec.2010.03.014, 2010.

Gosz, J. R., Brookins, D. G., and Moore, D. I.: Using strontium isotope ratios to estimate inputs to ecosystems, Bioscience, 33, 23-30, https://doi.org/10.2307/1309240, 1983.

Hobson, K. A., Barnett-Johnson, R., and Cerling, T.: Using Isoscapes to Track Animal Migration, in: Isoscapes: Understanding movement, pattern, and process on Earth through isotope mapping, edited by: West, J. B., Bowen, G. J., Dawson, T. E., and Tu, K. P., Springer Netherlands, Dordrecht, 273-298, https://doi.org/10.1007/978-90-481-3354-3_13, 2010.

Lech, M., Caritat, P. d., and McPherson, A.: National Geochemical Survey of Australia: Field Manual, 2007.

McNutt, R. H.: Strontium isotopes, in: Environmental tracers in subsurface hydrology, Springer, 233-260, https://doi.org/10.1007/978-1-4615-4557-6_8, 2000.

Moffat, I., Rudd, R., Willmes, M., Mortimer, G., Kinsley, L., McMorrow, L., Armstrong, R., Aubert, M., and Grün, R.: Bioavailable soil and rock strontium isotope data from Israel, Earth System Science Data, 12, 3641-3652, https://doi.org/10.5194/essd-12-3641-2020, 2020.

Nebel, O. and Stammeier, J. A.: Strontium isotopes, in: Encyclopedia of Geochemistry, Springer, 1379-1384, https://doi.org/10.1007/978-3-319-39312-4_137, 2018.

Ottesen, R., Bogen, J., Bølviken, B., and Volden, T.: Overbank sediment: a representative sample medium for regional geochemical mapping, Journal of Geochemical Exploration, 32, 257-277, https://doi.org/10.1016/0375-6742(89)90061-7, 1989.

Romaniello, S. J., Field, M. P., Smith, H. B., Gordon, G. W., Kim, M. H., and Anbar, A. D.: Fully automated chromatographic purification of Sr and Ca for isotopic analysis, J. Anal. At. Spectrom., https://doi.org/10.1039/c5ja00205b, 2015.

Scaffidi, B. K. and Knudson, K. J.: An archaeological strontium isoscape for the prehistoric Andes: Understanding population mobility through a geostatistical meta-analysis of archaeological 87Sr/86Sr values from humans, animals, and artifacts, Journal of Archaeological Science, 117, 105121, https://doi.org/10.1016/j.jas.2020.105121, 2020.

Voerkelius, S., Lorenz, G. D., Rummel, S., Quétel, C. R., Heiss, G., Baxter, M., Brach-Papa, C., Deters-Itzelsberger, P., Hoelzl, S., and Hoogewerff, J.: Strontium isotopic signatures of natural mineral waters, the reference to a simple geological map and its potential for authentication of food, Food chemistry, 118, 933-940, https://doi.org/10.1016/j.foodchem.2009.04.125, 2010.

Wilford, J.: A weathering intensity index for the Australian continent using airborne gamma-ray spectrometry and digital terrain analysis, Geoderma, 183, 124-142, https://doi.org/10.1016/j.geoderma.2010.12.022, 2012.

Willmes, M., Bataille, C. P., James, H. F., Moffat, I., McMorrow, L., Kinsley, L., Armstrong, R. A., Eggins, S., and Grün, R.: Mapping of bioavailable strontium isotope ratios in France for archaeological provenance studies, Applied Geochemistry, 90, 75-86, https://doi.org/10.1016/j.apgeochem.2017.12.025, 2018.

Willmes, M., McMorrow, L., Kinsley, L., Armstrong, R., Aubert, M., Eggins, S., Falguères, C., Maureille, B., Moffat, I., and Grün, R.: The IRHUM (Isotopic Reconstruction of Human Migration) database – bioavailable strontium isotope ratios for geochemical fingerprinting in France, Earth System Science Data, 6, 117-122, https://doi.org/10.5194/essd-6-117-2014, 2014.

https://doi.org/10.5194/essd-2025-277
Preprint. Discussion started: 10 June 2025

Open Access Earth System Science Data Discussions

Tables

Table 1. Environmental covariates used in the random forest model to predict bioavailable $^{87}Sr/^{86}Sr$ values.

No.	Variable Name	Description
1	r.m1	Global median of the bedrock $^{87}Sr/^{86}Sr$ isotope ratio model
2	r.srsrq1	First quartile (Q1) of the $^{87}Sr/^{86}Sr$ isotope ratio model
3	r.srsrq3	Third quartile (Q3) of the $^{87}Sr/^{86}Sr$ isotope ratio model
4	r.meanage_geol	Mean geological age of the bedrock (Myr)
5	r.minage_geol	Minimum geological age of the bedrock (Myr)
6	r.maxage_geol	Maximum geological age of the bedrock (Myr)
7	r.age	Global mean terrane (basement) age (Myr)
8	r.GUM	Global Unconsolidated Material (GUM) type
9	r.bouger	Bouguer gravity anomaly
10	r.elevation	Elevation above sea level (m)
11	r.mat	Mean annual temperature (°C)
12	r.map	Mean annual precipitation (mm/year)
13	r.ai	Aridity Index
14	r.pet	Potential evapotranspiration (mm/day)
15	r.dust	Dust deposition rate ($g/m^2/year$)
16	r.salt	Sea salt aerosol deposition ($g/m^2/year$)
17	r.distance	Distance to reference points (e.g. rivers or coasts)
18	r.volc	Volcanic sulfur deposition ($kg/m^2/s$)
19	r.fire	Black carbon from wildfires ($kg/m^2/s$)
20	r.foss	Black carbon from fossil fuels ($kg/m^2/s$)
21	r.clay	Soil clay content (%)
22	r.ph	Soil pH (converted to decimal)
23	r.cec	Cation exchange capacity ($cmol^+/kg$)
24	r.bulk	Soil bulk density (g/cm^3)
25	r.ocs	Organic carbon stock (kg/m^2)

https://doi.org/10.5194/essd-2025-277
Preprint. Discussion started: 10 June 2025

No.	Variable Name	Description
26	r.sw	Soil water content

References for each variable raster are listed in Bataille et al. (2020)

405

https://doi.org/10.5194/essd-2025-277
Preprint. Discussion started: 10 June 2025

Table 2. Summary of statistics of this study's 278 bioavailable $^{87}Sr/^{86}Sr$ ratios by region.

Region	**N**	**Min**	**Max**	**Mean**
N Aus	152	0.70501	0.78121	0.72150
SE Aus	38	0.70739	0.71908	0.71277
SW Aus	88	0.71153	0.75274	0.72468

Values represent the number of samples (N), minimum, maximum, and mean $^{87}Sr/^{86}Sr$ ratios for each region.

https://doi.org/10.5194/essd-2025-277
Preprint. Discussion started: 10 June 2025

410 **Figures**

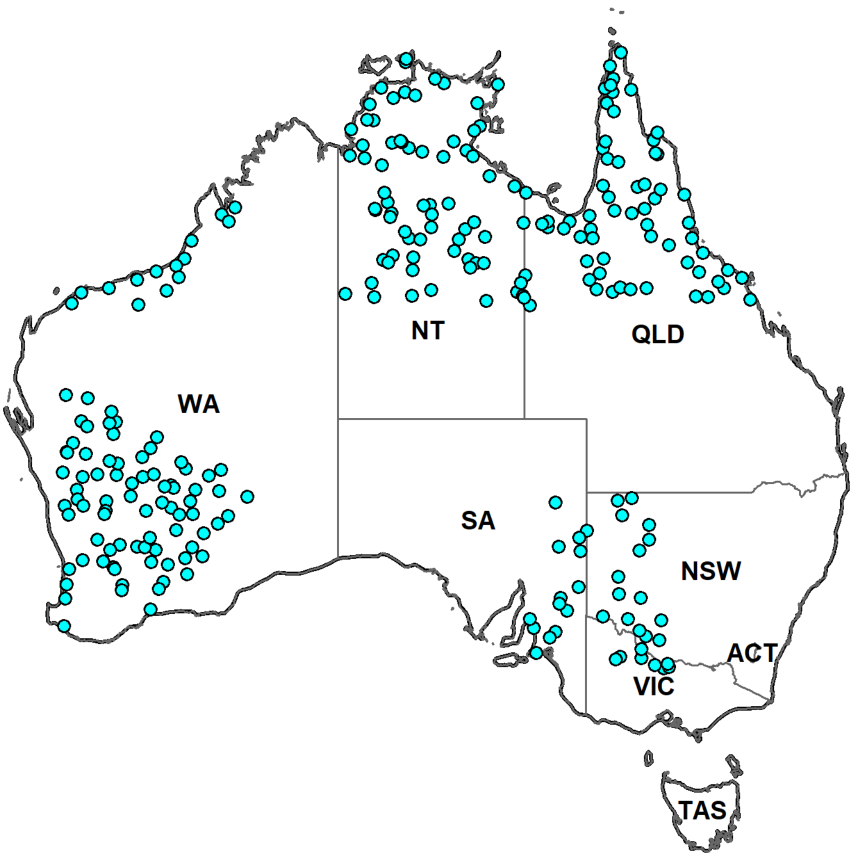

Figure 1. Map showing the locations of sediment samples analysed for bioavailable strontium (Sr) isotopes in this study (circles). Sampling sites span inland southeastern Australia (South Australia - SA, New South Wales - NSW, Victoria - VIC), northern Western Australia (WA), the Northern Territory (NT), Queensland (QLD) (north of 21.5°S), and the Yilgarn Craton in southern Western Australia.

https://doi.org/10.5194/essd-2025-277
Preprint. Discussion started: 10 June 2025

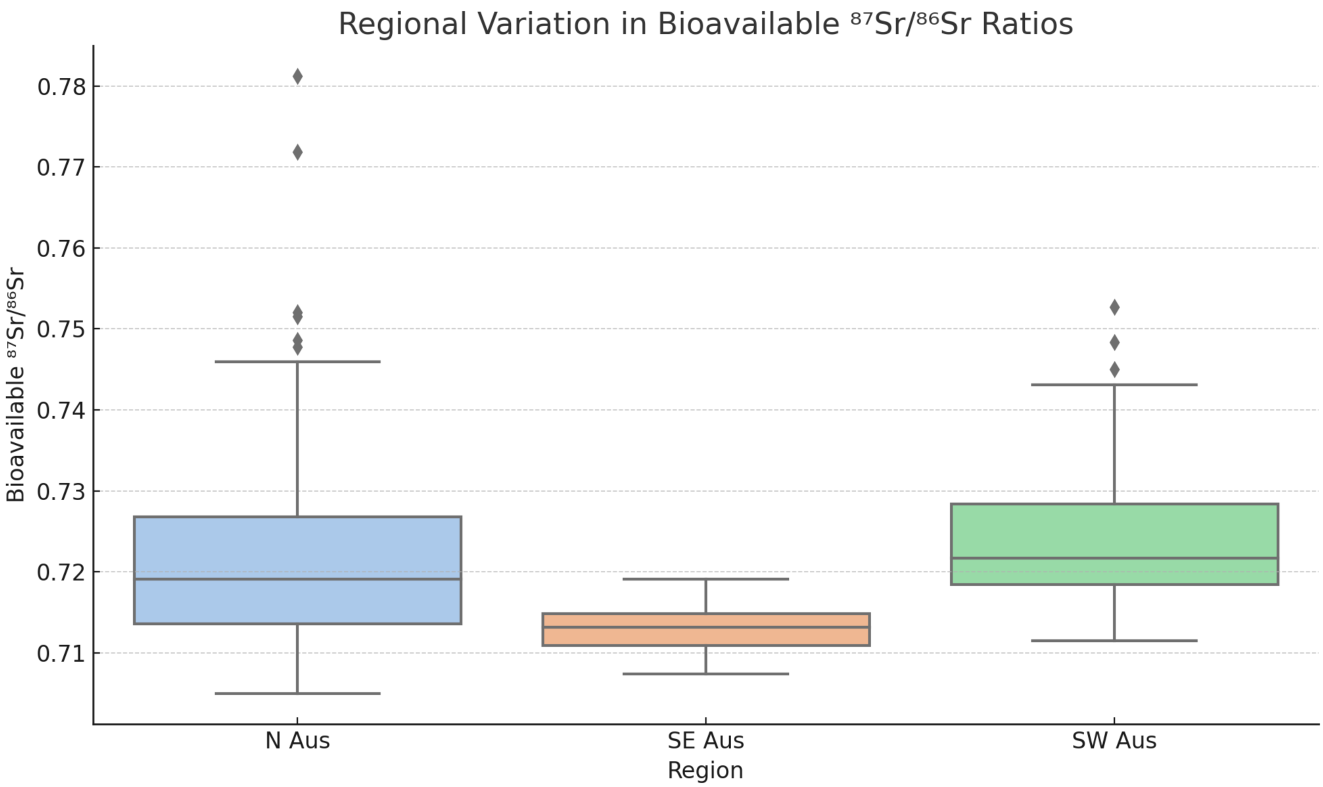

420 **Figure 2. Boxplot showing regional variation in bioavailable $^{87}Sr/^{86}Sr$ ratios across northern Australia (N Aus), southeastern Australia (SE Aus), and southwestern Australia (SW Aus). The data highlight systematic regional differences, with N Aus having the widest range of values, SE Aus displaying the lowest mean $^{87}Sr/^{86}Sr$ values, and SW Aus showing overall more radiogenic signatures (highest mean).**

https://doi.org/10.5194/essd-2025-277
Preprint. Discussion started: 10 June 2025

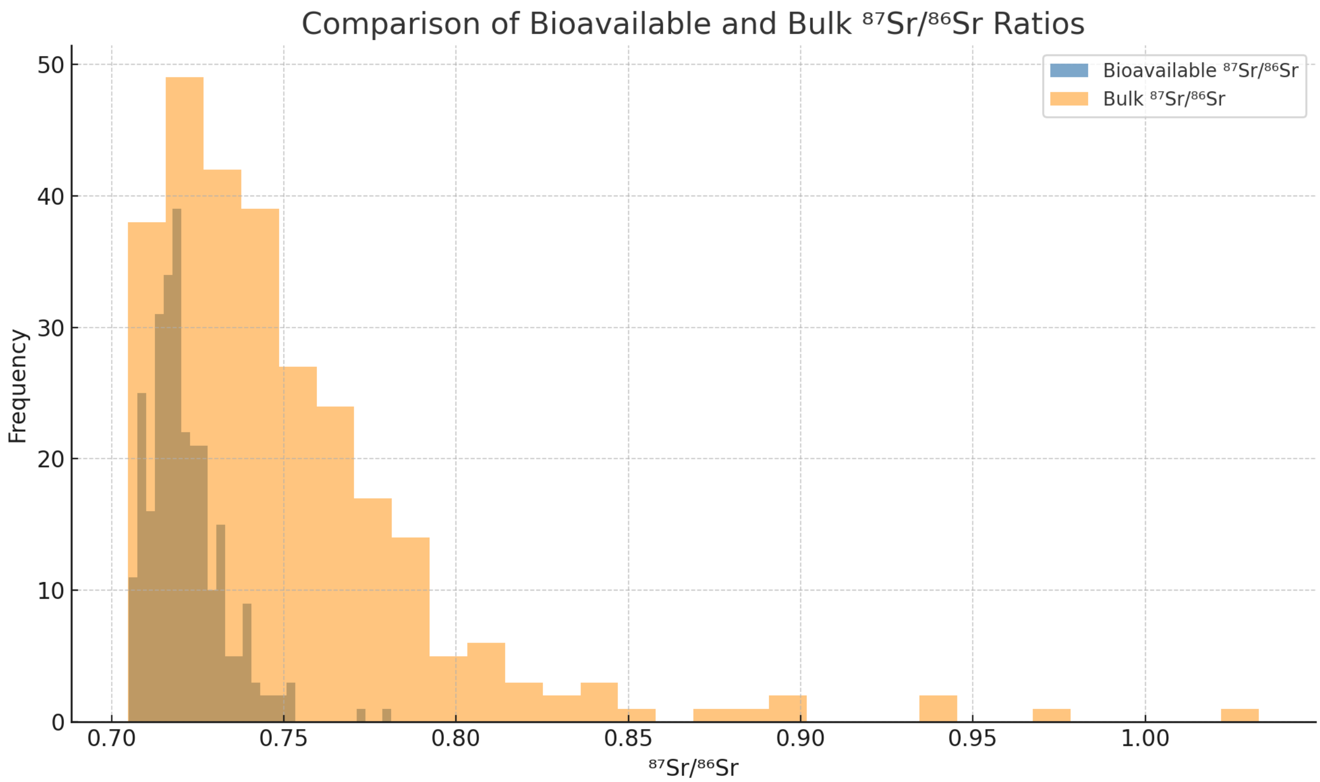

425 **Figure 3. Histogram comparing bioavailable (this study) and bulk $^{87}Sr/^{86}Sr$ ratios (Caritat et al., 2022, 2023, 2025b) across all samples. Bioavailable Sr (blue/grey; *n* = 278) displays a narrower and less radiogenic range, while bulk Sr (orange; *n* = 576) shows greater variability and extends to more radiogenic values. The broader range of bulk $^{87}Sr/^{86}Sr$ values reflects the inclusion of highly radiogenic minerals such as feldspars and micas within the bulk sediment, rather than being an artefact of the larger sample size compared to the bioavailable fraction.**

https://doi.org/10.5194/essd-2025-277
Preprint. Discussion started: 10 June 2025

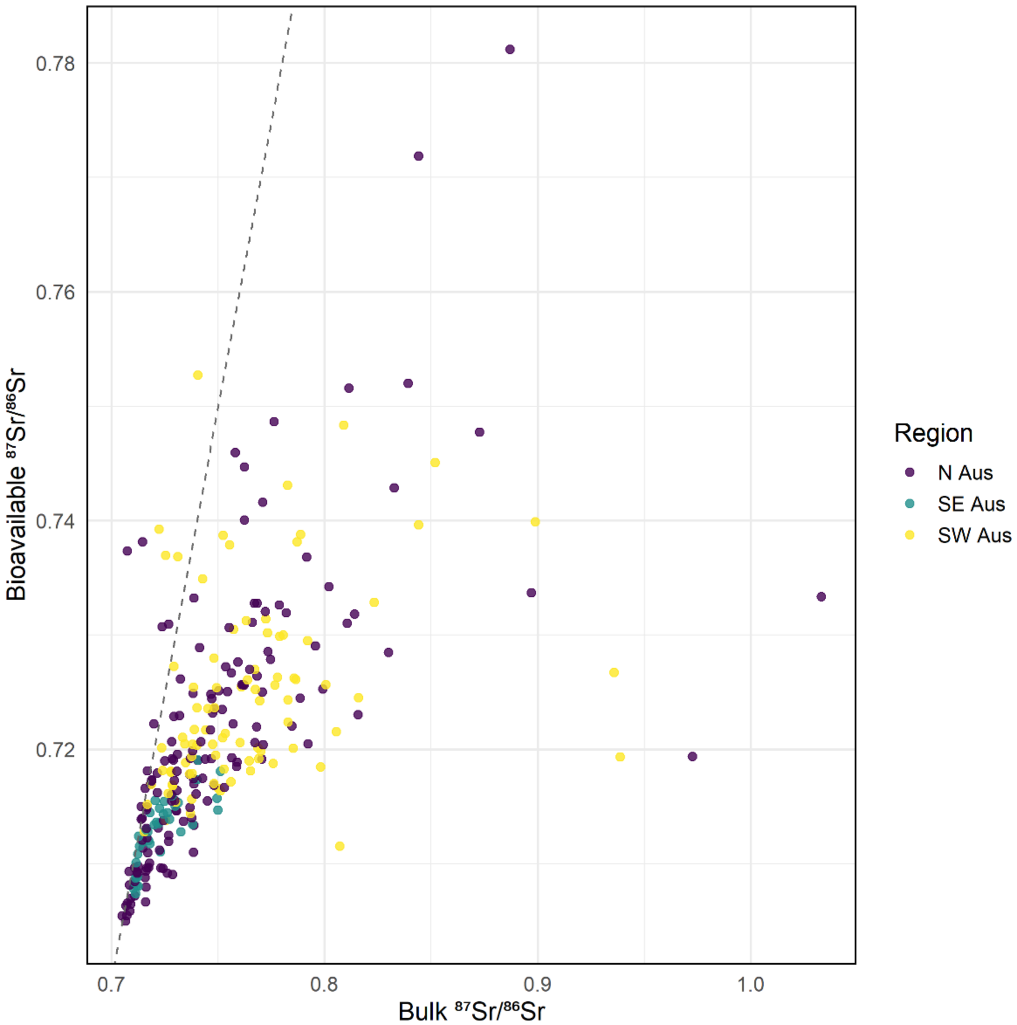

Figure 4. Relationship between bioavailable and bulk $^{87}Sr/^{86}Sr$ ratios for sediment samples across Australia. Points are coloured by region. The dashed line indicates a 1:1 relationship.

https://doi.org/10.5194/essd-2025-277
Preprint. Discussion started: 10 June 2025

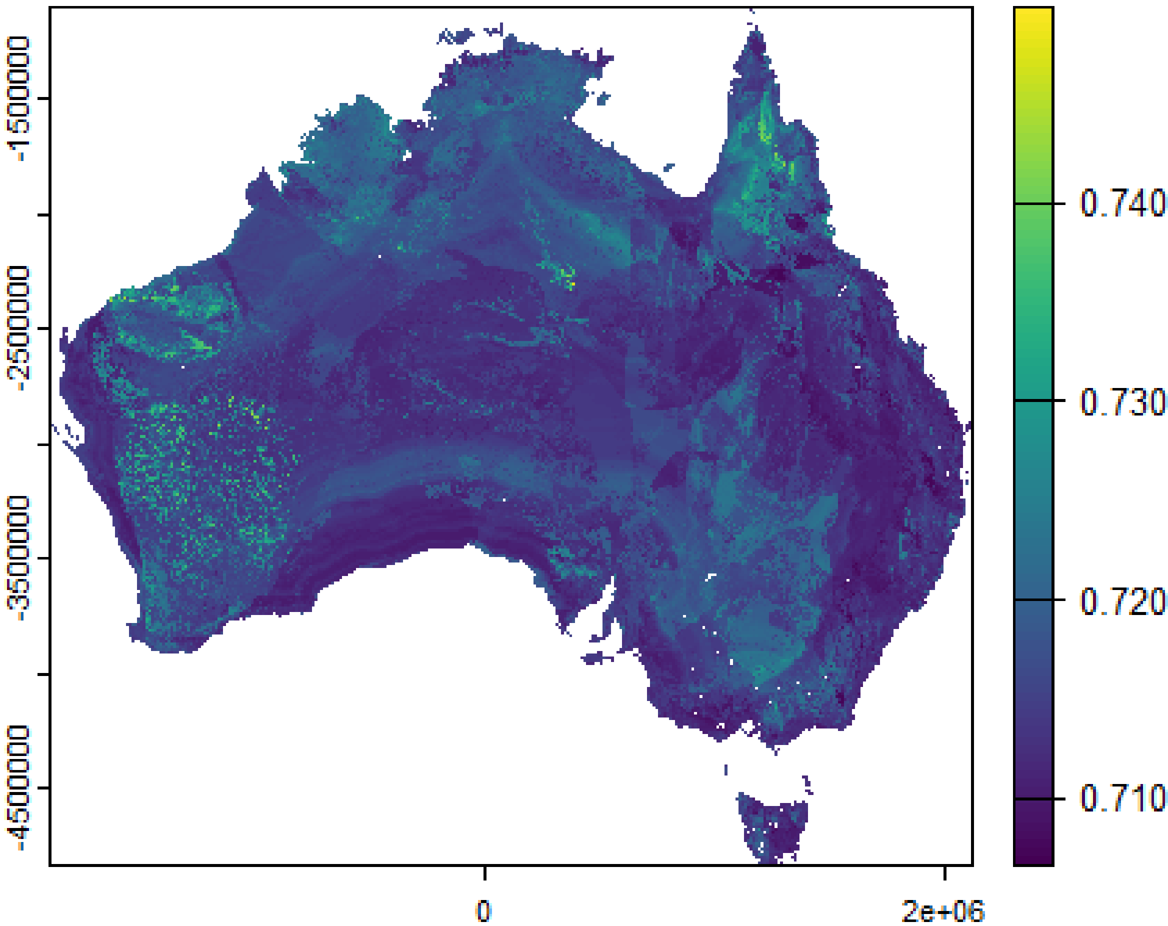

435 **Figure 5. Predicted bioavailable $^{87}Sr/^{86}Sr$ isoscape of Australia generated using a random forest regression model trained on 278 samples from this study and global reference datasets. The colour scale represents predicted bioavailable $^{87}Sr/^{86}Sr$ ratios, with lower values shown in purple and higher values in yellow. Higher predicted ratios are observed over ancient geological regions such as the Yilgarn Craton in Western Australia and parts of eastern Palaeozoic terranes. Lower values dominate younger sedimentary basins and coastal zones, reflecting geological age, regolith development, and potential marine or aeolian influences.**

440

https://doi.org/10.5194/essd-2025-277
Preprint. Discussion started: 10 June 2025

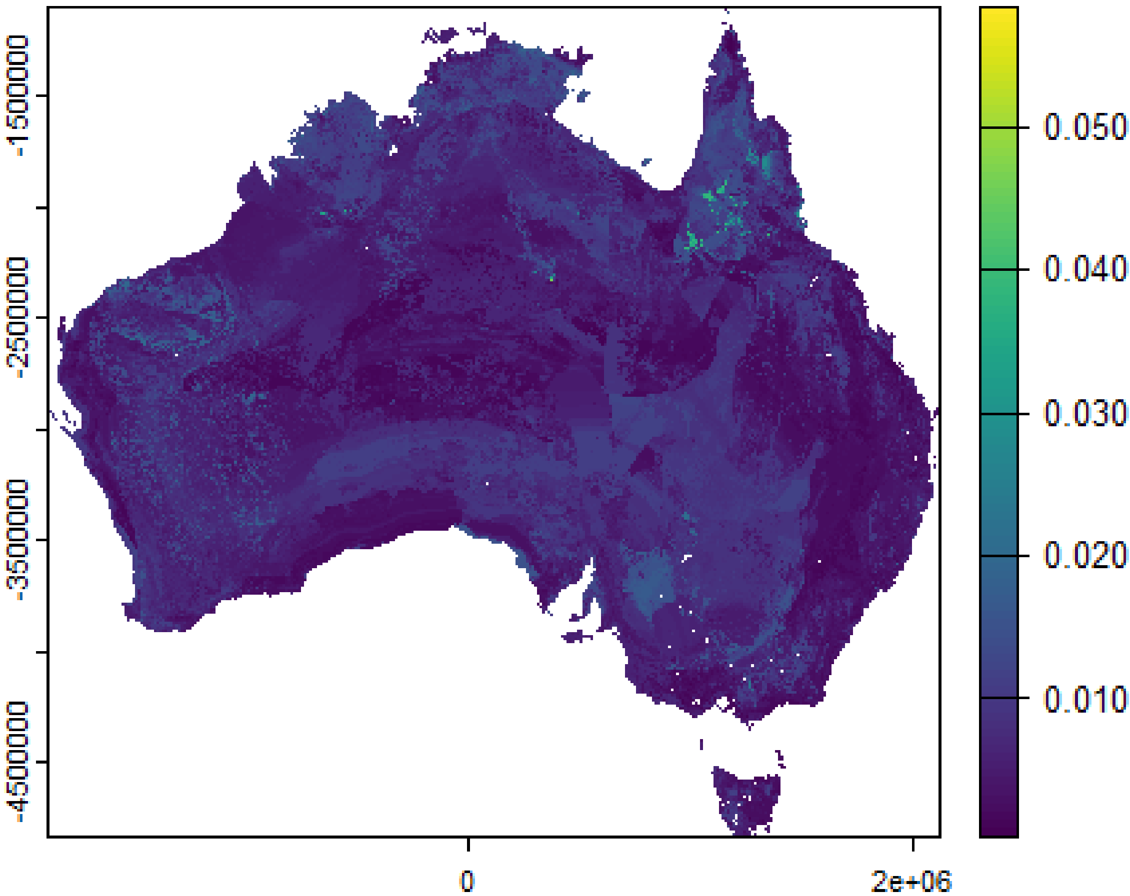

Figure 6. Map of the predicted uncertainty (standard deviation, SD) in bioavailable strontium isotope ratios ($^{87}Sr/^{86}Sr$) across Australia. Uncertainty values reflect the spatial prediction error estimated from the random forest model, based on input variables such as geology, precipitation, and dust sources. Higher SD values indicate lower confidence in the predicted $^{87}Sr/^{86}Sr$ ratios.

https://doi.org/10.5194/essd-2025-277
Preprint. Discussion started: 10 June 2025

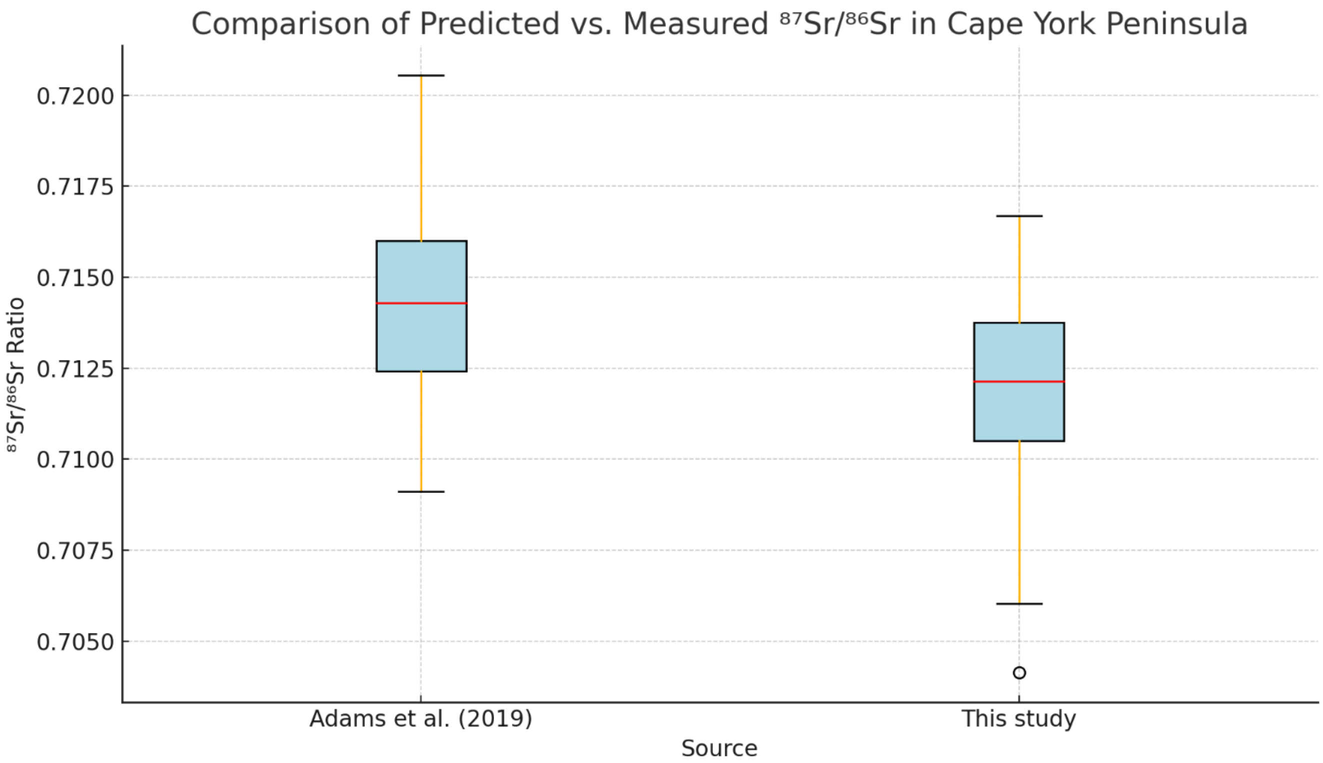

450 **Figure 7. Comparison of bioavailable $^{87}Sr/^{86}Sr$ ratios for the Cape York Peninsula between measured values reported by Adams et al. (2019) and predicted values from this study. The measured values are based on bioavailable Sr isotope ratios from plants, soils, and waters, while the predicted values were generated using a machine learning model trained on sediment samples and global reference datasets. Predicted values are lower than measured values by approximately 0.0025 but broadly capture the same isotopic range and spatial trends across Cape York.**